Journal of
MATERIALS RESEARCH

Welcome Comments Help

Improvement on the degradation of microwave sintered ZnO varistors by postannealing

Chang-Shun Chen
Department of Mechanical Engineering, HWA-HSIA College of Technology and Commerce, Taipei 235, Taiwan, Republic of China

Cheng-Tzu Kuo
Institute of Materials Science and Engineering, National Chiao-Tung University, Hsinchu 30050, Taiwan, Republic of China

I-Nan Lin
Materials Science Center, National Tsing-Hua University, Hsinchu 30043, Taiwan, Republic of China

(Received 25 September 1996; accepted 7 July 1997)

The microwave sintering process not only densified the ZnO materials in a higher rate, but also resulted in significantly better varistor characteristics. Large nonlinear coefficient and low leakage current density were attained by cooling the samples under a rate of 80 °C/min after sintering, followed by 600 °C postannealing for 60 min under oxygen atmosphere. Inappropriate annealing deteriorated the varistor characteristics that can either be attributed to the insufficient reoxidation along grain boundaries when annealed in N_2 (or air) or loss of Zn species in these regions when annealed at 750 °C (900 °C). By contrast, the degradation behavior of these materials can be improved by the annealing process regardless of the annealing atmosphere or temperature.

I. INTRODUCTION

The ZnO-based ceramics containing donors, sintering aids, and microstructural stabilizers[1–3] have been widely used as transient surge suppressors for protecting electrical circuits,[4,5] because of their highly nonlinear voltage (V)-current (I) characteristics and excellent surge-withstand capability. The non-ohmic properties of these materials are sensitive to the postsintering process even when the samples have been properly sintered,[6–8] which was attributed to the modification on the defect chemistry of the depletion region of the materials.

The degradation of varistor characteristics described by the increase in leakage current density with operation time is the behavior of prime concern in device applications, besides the non-ohmic property of the ZnO varistors.[9,10] Among the models proposed to account for the degradation mechanisms, the most acceptable one is due to Gupta and Carlson,[11] based on the migration of zinc interstitials present in the depletion region under the action of electric stress. Several approaches[8,11–15] have been attempted to improve the degradation behavior of ZnO varistors. Among them, heat treatment after sintering can effectively improve the stability of the materials,[16–18] which was assumed to result from the out diffusion of interstitial zinc (Zn_i).[19]

In this work, the donor-doped ZnO materials were densified by the microwave sintering process, since this process can enhance the densification rate for ceramic materials.[20–22] The effect of postsintering process, including the cooling rate and annealing conditions, on their varistor characteristics, especially the degradation behavior, will be examined. The possible mechanism for the modification of these properties is discussed.

II. EXPERIMENTAL PROCEDURES

A. Sample preparations

A typically commercial single uniform batch of ZnO varistor powders was prepared. The composition of the ZnO varistor samples consisted of 97 mol% ZnO with 1/2 mol% each of Bi_2O_3, Co_3O_4, TiO_2, and Cr_2O_3, and 1 mol% of Al_2O_3. The mixtures were ball-milled with a plastic jar, using zirconia balls and de-ionized water, for 8 h. They were then calcined at 750 °C in air for 2 h, followed by pulverization in a ball-mill for 8 h to around 0.8 μm size. The green compacts made of these powders were microwave sintering at 1000 °C for 10 min in an applicator made of WR284 waveguide, using a 2.45 GHz microwave generated from commercial source (Gerling GL107 magnetron). The temperature profile was measured using Pt-13% Rh thermocouple, placed near the sample surface. The heating rate was 40 °C/min and the cooling rate was either 145 °C/min, 80 °C/min, or 6 °C/min. For comparison, the samples were also prepared by a conventional sintering process, that is, sintering at 1000 °C for 60 min in an electrical furnace. The heating rate was 5 °C/min and the cooling rate was 1 °C/min, 5 °C/min, or fast cooled (~14 °C/min). In the annealing experiments, the microwave sintered samples, cooled by a rate of 80 °C/min, were either heat-

 © 1998 Materials Research Society

CAMBRIDGE JOURNALS
http://journals.cambridge.org Downloaded: 28 Apr 2014 IP address: 140.113.38.11

treated at 600 °C in controlled atmosphere (i.e., O_2, air or N_2) or heat-treated at 600–900 °C in O_2 atmosphere.

B. Measurements

The crystal structure and microstructure of the sintering samples were examined using a Rigaku D/mas-IIB x-ray diffractometer and JEOL JSM-840A scanning electron microscope (SEM), respectively. The average grain size, $\overline{G}$, was estimated with the linear intercept method as described by Mendelson[23] with a multiple factor of 1.56. The voltage-current (*V-I*) properties of these samples were measured using a Keithley 237 *I-V* electrometer after the silver paste was rubbed onto the sample surface and fired at 100 °C for 30 min to serve as electrodes. Breakdown voltage (V_{bk}) was evaluated from the *I-V* curve at a current density of 0.5 mA/cm^2, and the leakage current density (J_L) was estimated at a current density at 0.8 V_{bk}. The nonlinear coefficient (α) was calculated using the *I-V* properties of the materials in-between the current density ranges of 1.0 mA/cm^2 and 10 mA/cm^2. The capacitance-voltage (C-V) measurements were made at room temperature using H.P.4274A capacitance meter. The electrical characteristics, including barrier height (ϕ_b) and donor concentration (N_d), were determined from capacitance-voltage (*C-V*) data, using the model proposed by Mukae *et al.*[24] The capacitance-frequency relations were measured by a H.P. impedance analyzer (HP4194A). The degradation test was made at a temperature of 120 °C by monitoring the evolution of leakage current density with time, using a Keithley 237 I-V electrometer.

III. RESULTS AND DISCUSSIONS

A. Cooling rate effect

The sintering of ZnO materials needed only 1000 °C (10 min) to reach a high density as 96.0% T.D. (theoretical density) by microwave sintering process, whereas it took 1000 °C (60 min) to attain a similar density with the furnace sintering process. Phase constituents of the microwave sintered (ms) samples are not different from that of the furnace sintered (fs) ones. X-ray diffraction patterns shown in Fig. 1 indicate that they contain hexagonal ZnO as main constituents with Bi-rich phase ($24Bi_2O_3$–ZnO) and spinel as minor secondary phases. However, the microstructure of the ms-samples is significantly different from that of the fs-samples. Figure 2(a) shows that the ZnO materials densified by the furnace sintering process contained uniform grain size distribution, with the average grain size around 4 μm, which did not change with the cooling rate. By contrast, the grain size of the ms-samples is usually larger than that of the fs-samples, and the grains grew to a larger size when cooled in a slower rate, as shown in Figs. 2(b)–2(d). The grain size is around 5.6 μm for ms-samples cooled with 145 °C/min and is about 6.9 μm for those cooled with 6 °C/min. Moreover, abnormal grain growth occurred for the ms-samples slowly cooled [Fig. 2(d)], inferring that the diffusivity of the ions is still during this period.

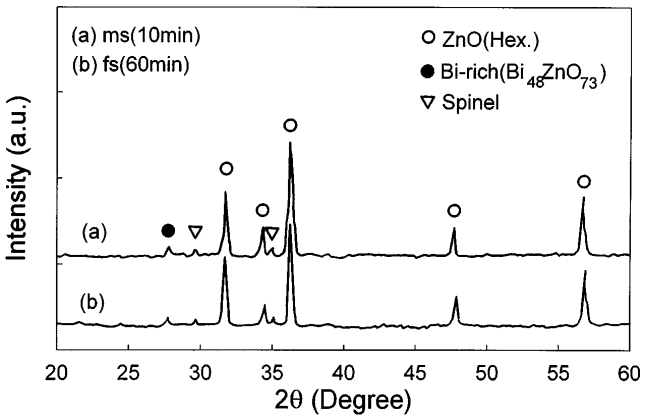

FIG. 1. The x-ray diffraction patterns of ZnO materials densified by (a) furnace sintering process at 1000 °C for 60 min and (b) microwave sintering process at 1000 °C for 10 min.

Cooling rate modified the electric field-current density (J-E) characteristics of the fs-samples only moderately. Figure 3(a) shows that the leakage current density (J_L) varied in-between (J_L) = 2.2×10^{-5}–4.6×10^{-5} A/cm^2, the nonlinear coefficient (α value) changed in-between α = 30–26, and the breakdown voltage (V_{bk}) is around V_{bk} = 343–307 V/mm. Moreover, the capacitance-voltage (*C-V*) measurement revealed that the potential barrier height (ϕ_b) and the donor concentration (N_d) of these samples also changed insignificantly with the cooling rate, that is, ϕ_b = 3.05–2.25 eV and $N_d = 10.9 \times 10^{24}$–$8.6 \times 10^{24}$ m^{-3}, as shown in Fig. 3(b) and Table I(a).

On the contrary, a sufficiently large cooling rate, i.e., $r > 80$ °C/min, is needed in the microwave sintering process to keep the varistor characteristics unmodified. The cooling rate from 145 °C/min to 80 °C/min only moderately changed the material's properties, that is, $J_L = 7.0 \times 10^{-5}$–5.3×10^{-5} A/cm^2, V_{bk} = 100–110 V/mm, α =25–27, ϕ_b = 0.82–0.87 eV, $N_d = 15.1$–13.5×10^{24} m^{-3}. However, lowering the cooling rate from 80 °C/min to 6 °C/min increased the leakage current density abruptly from $J_L = 5.3 \times 10^{-5}$ A/cm^2 to $J_L = 30.0 \times 10^{-5}$ A/cm^2 and lowered the nonlinearity from α = 27 to α = 7, and accompanied with the decrease of the potential barrier height from ϕ_b = 0.87 to ϕ_b = 0.73 and the breakdown voltage from V_{bk} = 110 to 32 V/mm, as indicated in Fig. 4 and Table I(b). This is attributed to the fact that, when ZnO materials were cooled in a rate of 6 °C/min, they remained at high

CAMBRIDGE JOURNALS
http://journals.cambridge.org Downloaded: 28 Apr 2014 IP address: 140.113.38.11

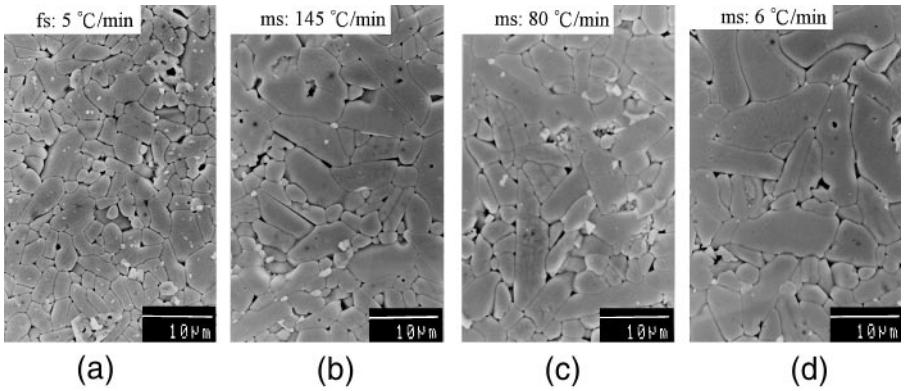

FIG. 2. The SEM micrographs of ZnO materials densified by (a) the furnace sintering process (1000 °C, 60 min) and cooled in a rate of 5 °C/min, and those sintered by the microwave sintering process (1000 °C, 10 min) and cooled in a rate of (b) 145 °C/min, (c) 80 °C/min, and (d) 6 °C/min.

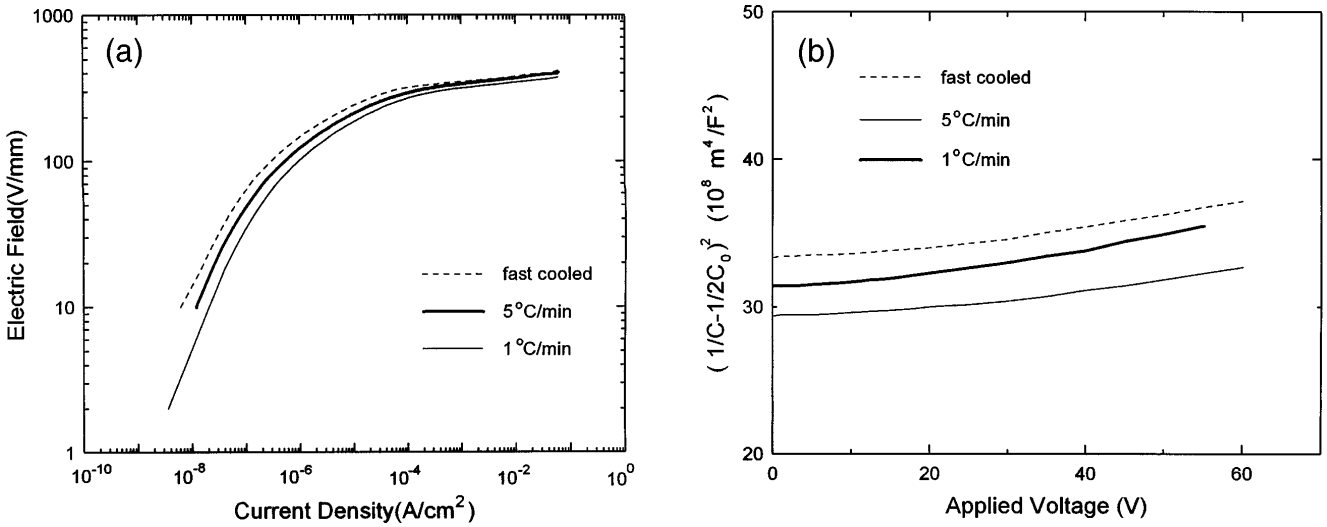

FIG. 3. The (a) electric field-current density (E-J) and (b) the capacitance-voltage (C-V) properties of ZnO materials densified by the furnace sintering process (1000 °C, 60 min) and cooled with various rates (fast cooled ~14 °C/min).

TABLE I. Cooling rate effect on varistor characteristics of ZnO materials: (a) furnace sintered and (b) microwave sintered.

Sintering process	Cooling rate (°C/min)	V_{bk} (V/mm)	J_L (10^{-5} A/cm^2)	α	ϕ_b (eV)	N_d (10^{24}/m^3)	Grain size (μm)
(a) FS:	fast cooled	343	2.2	30	3.05	10.9	4.0
	5	331	3.6	28	2.64	10.7	4.0
	1	307	4.6	26	2.25	8.6	4.1
(b) MS:	145	100	7.0	25	0.82	15.1	5.6
	80	110	5.3	27	0.87	13.5	5.9
	6	32	30.0	7	0.73	19.8	6.9

Fast cooled: >14 °C/min for 1000 °C–800 °C; 5 °C/min for 800 °C–500 °C.
FS: furnace sintering 1000 °C (60 min); MS: microwave sintering 1000 °C (10 min).

temperature for such a long period that induced abnormal grain growth, and accompanied by the loss of ZnO species along grain boundary regions. It should be noted that the time interval needed for samples to cool from 1000 °C to 940 °C (~10 min) is comparable with the sintering period in microwave sintering process.

As indicated in Tables I(a) and I(b), the microwave sintering process resulted in significantly lower work function (ϕ_b), larger donor concentration (N_d), and larger leakage current density (J_L) than the furnace sintering process. The modification on the varistor characteristics of the ZnO materials due to the change in sintering process is, apparently, closely related to the modification on the defect chemistry in depletion region near the grain boundaries, since the change mainly occurred at the prebreakdown region of the J-E curve, with

CAMBRIDGE JOURNALS
http://journals.cambridge.org Downloaded: 28 Apr 2014 IP address: 140.113.38.11

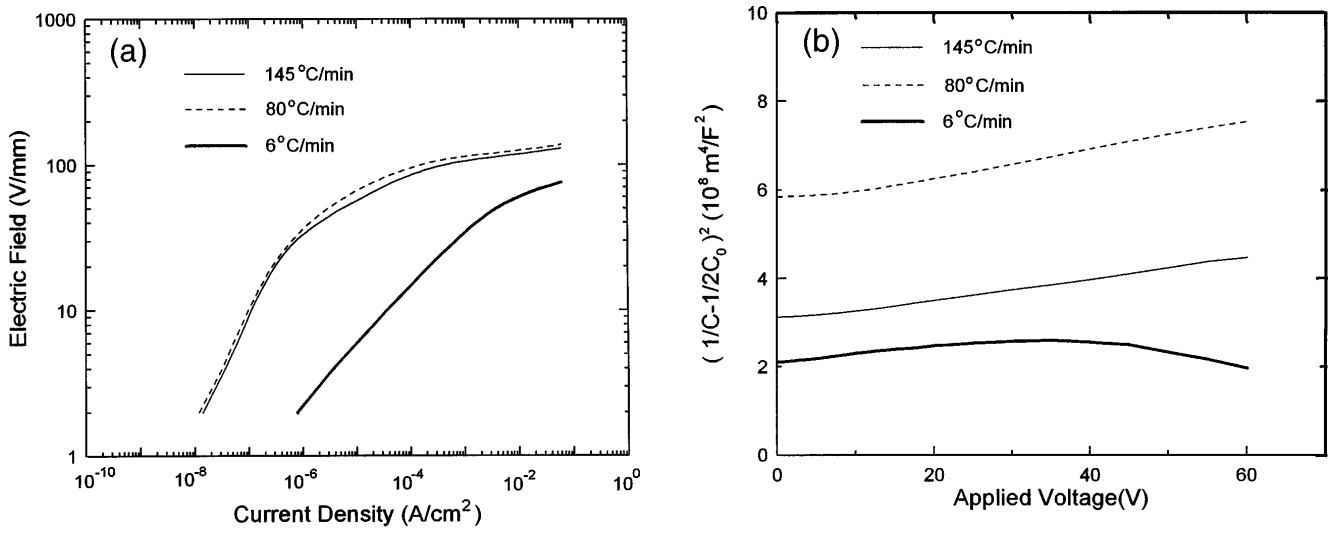

FIG. 4. The (a) electric field-current density (E-J) and (b) the capacitance-voltage (C-V) properties of ZnO materials densified by the microwave sintering process (1000 °C, 10 min) and cooled with various rates.

the upturn region remaining unaffected. The potential barrier height of the materials is related to the donor concentration (N_d) and surface states (N_s) with the following relationship[19,24]:

$$\phi_b = q^2 N_s^2 / 2\epsilon\epsilon_0 N_d, \quad (1)$$

where q and ϵ_0 are the electronic charges and dielectric constant of vacuum, respectively; ϵ is the relative dielectric constant of the materials. The donors are either the trivalent donor dopants (i.e., Sb^{3+}), the interstitial Zn species (i.e., Zn_i), or the oxygen vacancies (V_O), whereas the surface states may be contributed by the impurities or adsorpted oxygen at grain boundaries and the effective trap level induced by the cation vacancies (i.e., V_{Zn}) presented in depletion region. Larger donor density contained in ms-samples can be attributed to the freezing of excess interstitial Zn species formed at high temperature by the fast cooling process. However, it is believed that the grain boundaries of the microwave sintered materials are less defective, i.e., contained smaller proportion of surface states, which is the more important cause of the lowering of the ϕ value of those samples. These phenomena, however, required more detailed investigation.

The dielectric properties of the ZnO varistors are strongly frequency dependent. As shown in Fig. 5(a), the apparent dielectric constant decreased monotonously with the measuring frequencies. The K value of the microwave sintered (ms) samples, $K_{ms} = 3000–4000$ at 1 kHz, is larger than that of the conventional furnace sintered (fs) samples, i.e., $K_{fs} = 1000$ at 1 kHz. These dielectric constant values are exceedingly larger than that of the pure ZnO materials ($K_{ZnO} = 8.5$), indicating that the ZnO varistors behaved as a grain boundary barrier layer (GBBL) capacitors, which possessed unique microstructure as semiconducting grains separated by insulating grain boundaries. Similar characteristics are even more clearly illustrated in the frequency dependence of dissipation factor [Fig. 5(b)]. A noteworthy dielectric relaxation peak occurred in the vicinity of 300 kHz for ms-samples and in the vicinity of 3 MHz for fs-samples. The low frequency resonance at 300 kHz can apparently be attributed to the relaxation of space charge polarization (SCP), which occurred for electrons to transport inside the grain interior, in between the grain boundary barriers, whereas the high frequency resonance at 3 MHz can be ascribed to the relaxation of the orientational polarization (OP) in the depletion region of the ZnO materials, according to the "valence electron resonance model" proposed by Alim[25] or Shim and Cordaro,[26,27] where the electrons were assumed to hop in-between the intrinsic defects with ~0.33 eV trap level. The SCP relaxation was suppressed in fs-samples due to low N_d and small grain characteristics of these materials. On the other hand, the OP relaxation, which should also occur to ms-samples, is not observable due to the appearance of the exceedingly large SCP-resonance peak and relatively small OP-resonance peak, due to thinner depletion region (i.e., small ϕ_b) of these materials. A large proportion of equivalent donor concentration (N_d), the interstitial Zn, induced in microwave sintering process, in addition to the thinner depletion region near the grain boundaries, can account for the larger apparent dielectric constant of ms-samples.

B. Annealing effect

The degradation of the ZnO materials, which is the change of their electrical properties with time, is another

CAMBRIDGE JOURNALS
http://journals.cambridge.org Downloaded: 28 Apr 2014 IP address: 140.113.38.11

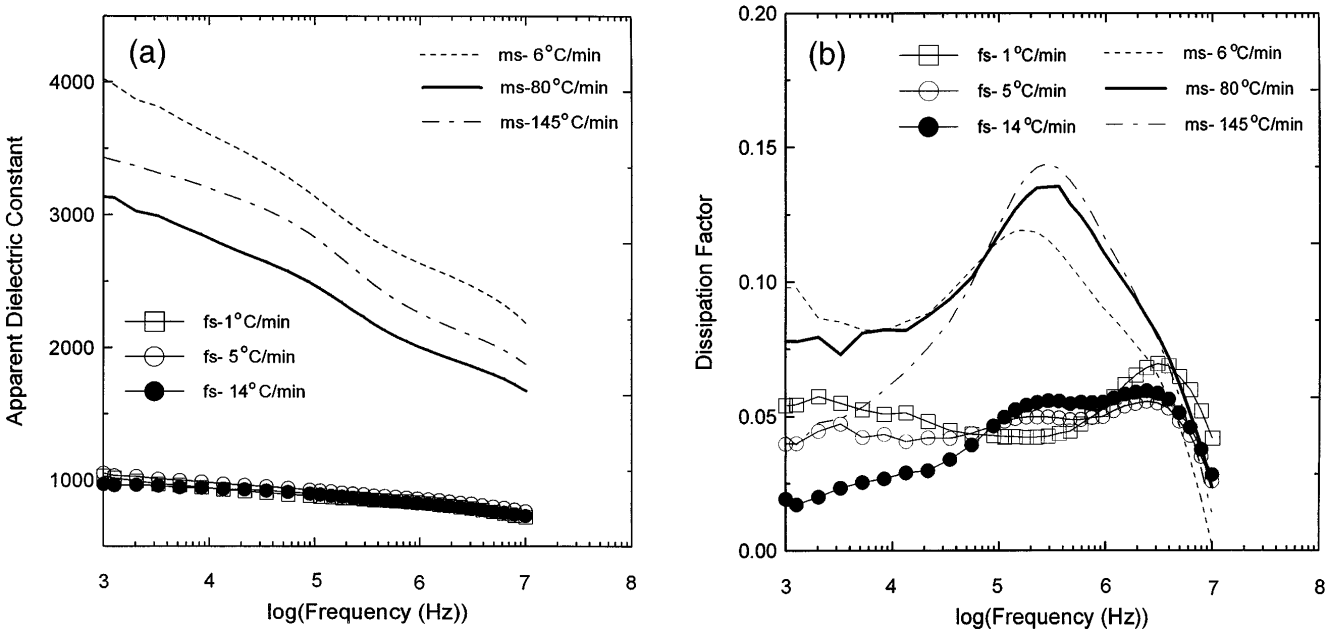

FIG. 5. The effect of cooling rate on frequency dependence of (a) apparent dielectric constant and (b) dissipation factor of ZnO varistors.

characteristic of prime importance for the application of varistor devices. It was proposed that the degradation of ZnO materials was induced by the out diffusion of interstitial Zn atom under electric stress and can be markedly improved by annealing these materials under oxidizing atmosphere at 600–800 °C.[10] Similar experiments were thus performed on the microwave sintered samples (1000 °C, 10 min and 80 °C/min) to examine the annealing effect on their degradation behavior.

The electric field-current density (E-J) and capacitance-voltage (*C-V*) behaviors of the 600 °C annealed ms-samples are shown in Figs. 6(a) and 6(b), respectively, and the corresponding varistor characteristics deduced from these curves are listed in Table IIa. It is observed that annealing in either air or nitrogen atmosphere at 600 °C deteriorated the varistor behavior markedly; that is, the leakage current density increased from $J_L = 5.3 \times 10^{-5}$ A/cm^2 to $J_L = 9.8$–18×10^{-5} A/cm^2 and the nonlinearity decreased from $\alpha = 27$ to $\alpha = 11$–8 after annealing, the potential barrier height increased from $\phi_b = 0.87$ eV to $\phi_b = 1.10$ eV, while the donor concentration was not significantly changed. Contrarily, annealing in oxygen atmosphere at 600 °C lowered the leakage current density significantly to $J_L = 1.5 \times 10^{-5}$ A/cm^2, maintaining the other varistor characteristics unaltered. On the other hand, the leakage current density for the ZnO samples, normalized by the initial leakage current density (J_0), increased pronouncedly with time for the as-sintered samples [fine solid curve, Fig. 6(c)] and the degradation behavior was substantially suppressed due to the annealing process, regardless of annealing atmosphere. Although the annealing in N_2 atmosphere resulted in large initial leakage current density (J_0), this value will not further increase with time [dash-dotted curve, Fig. 6(c)].

It was proposed that the prime reactions occurred during annealing process are the inward diffusion of oxygen along the grain boundary region and the outward diffusion of Zn-interstitials from grain interior to the boundary region.[3] The former will annihilate the oxygen vacancies that reduced the effective donor concentration via the following reaction:

$$1/2\ \mathrm{O}_2(\mathrm{g}) + \mathrm{V}_\mathrm{O} = \mathrm{O}_\mathrm{O}(\mathrm{g.b}), \qquad (2)$$

and, therefore, lowered the leakage current density. The increase in leakage current density, when the samples were annealed in air or N_2 atmosphere, can thus be ascribed to the insufficient supply of the oxygen. An abundance of oxygen vacancies was thus induced. On the other hand, outward diffused Zn-interstitials will interacted with the Zn-vacancies, V_{Zn}, via the following reaction:

$$V_{\mathrm{Zn}} + \mathrm{Zn}_i = \mathrm{Zn}_{\mathrm{Zn}} + V_i \qquad (3)$$

and then recombined with oxygen species incorporated into the lattice via the reaction described in Eq. (2). Simultaneous elimination of the Zn interstitials (Zn_i) and Zn vacancies (V_{Zn}) did not alter the materials' varistor characteristics, since the effective donor concentration (N_d) was not altered. However, the degradation behavior of these materials, which occurred due to the diffusion of Zn_i species under the electric stress, was significantly

CAMBRIDGE JOURNALS
http://journals.cambridge.org Downloaded: 28 Apr 2014 IP address: 140.113.38.11

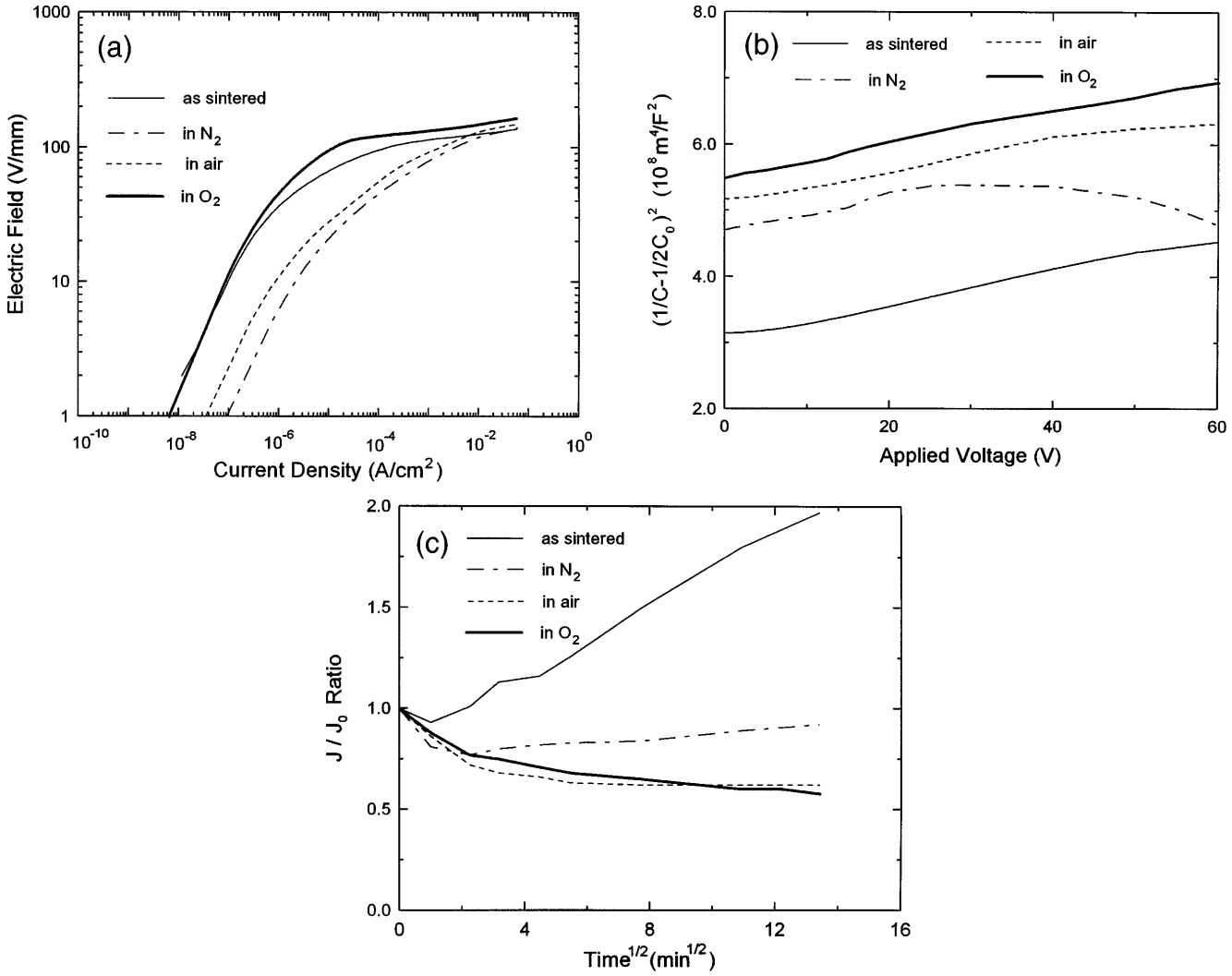

FIG. 6. The effect of annealing atmosphere (N_2, air, or O_2, 600 °C) on (a) J-E, (b) C-V, and (c) degradation of leakage current density of the ZnO materials microwave sintered at 1000 °C, 10 min, followed by cooled in 80 °C/min.

TABLE II. Annealing effect on varistor characteristics of ZnO materials: (a) atmospherical effect and (b) temperature effect.

Annealing conditions	V_{bk} (V/mm)	J_L (10^{-5} A/cm^2)	α	ϕ_b (eV)	N_d (10^{24}/m^3)
(a) 600 °C in N_2	82	18	8	1.10	13.6
600 °C in air	120	9.8	11	1.16	13.3
600 °C in O_2	129 (110)	1.5 (5.3)	29 (27)	1.20 (0.87)	12.5 (13.5)
(b) 750 °C in O_2	115	5.0	20	1.03	5.69
900 °C in O_2	90	4.9	19	0.86	5.27

(. . .) properties of as-sintered ZnO materials.

improved [cf. Fig. 6(c)]. The assumption that the elimination of Zn_i species improves the degradation behavior of these materials is in accord with the mechanism reported earlier.[3] Restated, annealing in oxidizing atmosphere, i.e., O_2, not only suppressed the initial leakage current density (J_0) but also improved the degradation behavior [bold solid curve, Fig. 6(c)], which ascribed to the annihilation of Zn-interstitials and oxygen vacancies.

On the other hand, annealing in oxygen at higher temperature (i.e., 750 and 900 °C) deteriorated the varistor characteristics markedly. The nonlinear coefficient (α) and the donor concentration (N_d) were significantly

CAMBRIDGE JOURNALS
http://journals.cambridge.org Downloaded: 28 Apr 2014 IP address: 140.113.38.11

lowered, while the leakage current density (J_L), the potential barrier height (ϕ_b), and breakdown voltage (V_{bk}) were insignificantly altered, as shown in Fig. 7 and Table II(b). However, the degradation of the leakage current density was still improved, even though the varistor characteristics were markedly degraded. These phenomena indicate, again, that the degradation behavior is intimately related to the presence of a large proportion of interstitial Zn species existing in the grain interior, whereas the other varistor characteristics are more closely related to the constitution and proportion of atomic defects existing in the depletion zone near the grain boundaries.

Postannealing at 600 °C imposed an insignificant effect on the dielectric properties of the ZnO varistors, regardless of annealing atmosphere. As shown in Figs. 8(a) and 8(b), the apparent dielectric constant decreased monotonously with measuring frequency and an SCP relaxation occurred in the vicinity of 300 KHz. Postannealing at higher temperature (i.e., 750 and 900 °C, O_2) markedly lowered the apparent dielectric constant and suppressed the space charge polarization (SCP) relaxation. Table II inferred, again, that the decrease in donor concentration (N_d) is the main factor resulting in the modification on the dielectric properties.

IV. CONCLUSIONS

Sintering behavior and varistor characteristics of ZnO materials prepared by microwave or furnace sintering process were examined. The ZnO samples can be densified to >96% T.D. (theoretical density) at 1000 °C (10 min) in the microwave sintering process and at 1000 °C (60 min) in the furnace sintering process. Cooling rate after sintering markedly modified the microstructure, electric field-current density (*J-E*), and

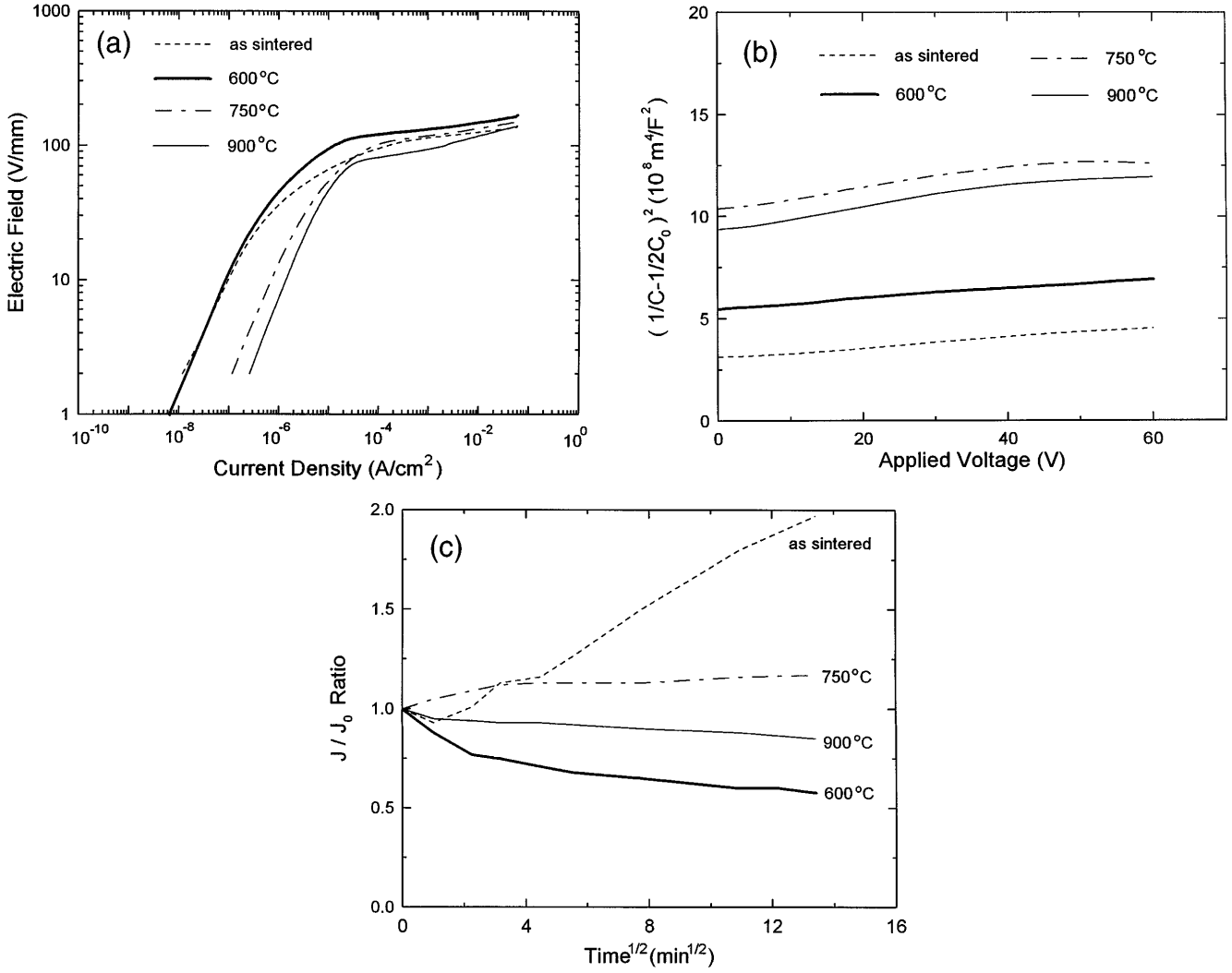

FIG. 7. The effect of annealing temperature (600 °C, 750 °C, or 900 °C, in O_2) on (a) J-E, (b) C-V, and (c) degradation of leakage current density of the microwave sintered ZnO materials.

CAMBRIDGE JOURNALS
http://journals.cambridge.org Downloaded: 28 Apr 2014 IP address: 140.113.38.11

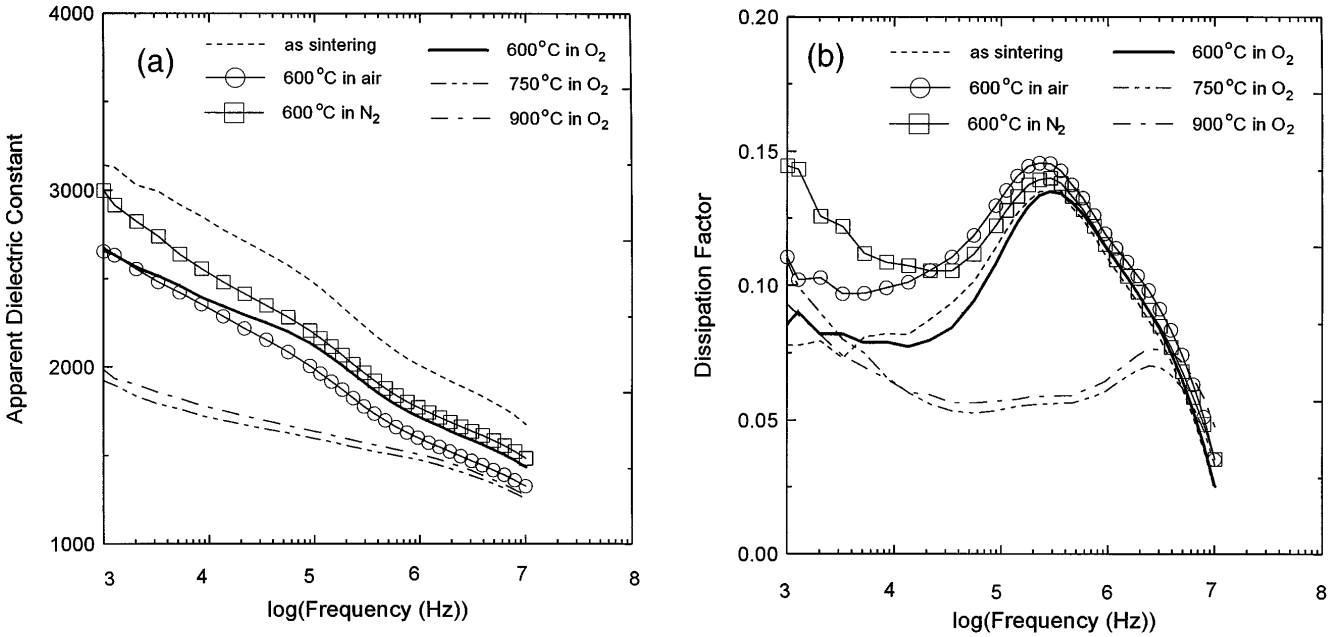

FIG. 8. The effect of postannealing on frequency dependence of (a) apparent dielectric constant and (b) dissipation factor of ZnO varistors.

capacitance-voltage (*C-V*) characteristics of the microwave sintered samples, but insignificantly altered those properties of the furnace sintered samples.

Postannealing resulted in a pronounced effect on both the varistor characteristics and the degradation behavior of ZnO materials. Annealing under O_2 atmosphere at 600 °C for 1 h optimized the varistor properties, with leakage current density $J_L = 1.5 \times 10^{-5}$ A/cm^2, nonlinear coefficient $\alpha = 29$, and breakdown voltage $V_{bk} =$ 129 V/mm, and the intrinsic parameters with potential barrier height $\phi_b = 1.20$ eV and donor concentration $N_d = 1.33 \times 10^{25}$ m^{-3}. Annealing under nonoxidizing atmosphere (air and N_2) and unsuitable temperature (750 or 900 °C) deteriorated the varistor characteristics that were ascribed to the insufficient reoxidation or the induction of oxygen and zinc vacancies. Contrarily, the degradation behavior, evaluated by time evolution of leakage current density, was significantly improved by the annealing process, regardless of annealing atmosphere or temperature. Such a behavior was attributed to the elimination of interstitial zinc (Zn_i) due to annealing such that the phenomenon of out diffusion of Zn_i species was suppressed.

ACKNOWLEDGMENT

Financial support by National Science Council of the Republic of China through Grant No. NSC 85-2216-E007-040 was gratefully acknowledged by the authors.

REFERENCES

1. M. Matsuoka, Jpn. J. Appl. Phys. **10**, 736 (1972).
2. L. M. Levinson and H. R. Philipp, Am. Ceram. Soc. Bull. **65**, 639 (1986).
3. T. K. Gupta, J. Am. Ceram. Soc. **73**, 1817 (1990).
4. K. Eda, J. Appl. Phys. **49**, 2964 (1978).
5. P. R. Emtage, J. Appl. Phys. **48**, 4372 (1977).
6. N. Raghu and T. R. N. Kutty, Appl. Phys. Lett. **60**, 100 (1992).
7. E. Olsson, G. Dunlop, and R. Osterlund, J. Am. Ceram. Soc. **76**, 65 (1993).
8. J. M. Wu and J. J. Shyu, J. Mater. Sci. **24**, 1881 (1989).
9. H. R. Philipp and L. M. Livinson, in *Advances in Ceramics*, edited by M. F. Yan and A. H. Heuer (American Ceramic Society, Westerville, OH, 1983), Vol. 7, p. 30.
10. E. Sonder, M. M. Austin, and D. L. Kinser, J. Appl. Phys. **54**, 3566 (1983).
11. T. K. Gupta and G. W. Carlson, J. Mater. Sci. **20**, 3487 (1985).
12. T. K. Gupta and G. W. Carlson, J. Appl. Phys. **53**, 7401 (1982).
13. A. Iga, M. Matsuoka, and T. Masuyama, Jpn. J. Appl. Phys. **15**, 1847 (1976).
14. T. K. Gupta and A. C. Miller, J. Mater. Res. **3**, 745 (1988).
15. K. Eda, in *Ceramic Transactions*, edited by L. M. Levinson (American Ceramic Society, Westerville, OH, 1989), Vol. 3, p. 10.
16. A. Iga, M. Matsuoka, and T. Masuyama, Jpn. J. Appl. Phys. **15**, 1161 (1976).
17. N. Shohata and J. Yoshida, Jpn. J. Appl. Phys. **16**, 2299 (1977).
18. M. Inada, Jpn. J. Appl. Phys. **18**, 1439 (1979).
19. K. Eda, A. Iga, and M. Matsuoka, J. Appl. Phys. **51**, 2678 (1980).
20. W. H. Sutton, Bull. Am. Ceram. Soc. **68**, 376 (1989).
21. M. A. Janney, C. L. Calhoum, and H. D. Kimery, J. Am. Ceram. Soc. **75**, 341 (1992).
22. C-S. Chen, C-T. Kuo, and I-N. Lin, Jpn. J. Appl. Phys. **35**, 4696 (1996).
23. M. I. Mendelson, J. Am. Ceram. Soc. **52**, 443 (1969).
24. K. Mukae, K. Tsuda, and I. Nagasawa, J. Appl. Phys. **50**, 4475 (1979).
25. M. A. Alim, J. Am. Ceram. Soc. **72**, 28 (1989).
26. L. M. Levinson and H. R. Philipp, J. Appl. Phys. **47**, 1117 (1976).
27. Y. Shim and J. F. Cordaro, J. Am. Ceram. Soc. **71**, 184 (1988).

CAMBRIDGE JOURNALS
http://journals.cambridge.org Downloaded: 28 Apr 2014 IP address: 140.113.38.11